Tech Science Press

Characterization of Bacterial Cellulose From Oil Palm Shoot Juices and Coconut Juice/Poly(ethylene glycol) Biocomposite

Nantharat Phruksaphithak[1,*], Chalermkiet Kaewnun[2] and Sompong O-Thong[2]

[1]Department of Chemistry, Faculty of Science, Thaksin University, Phatthalung, 93210, Thailand.

[2]Biotechnology program, Microbial Resource Management Research Unit, Department of Biology, Microbial Resource Management Research Unit, Faculty of Science, Thaksin University, Phatthalung, 93210, Thailand.

[*]Corresponding Author: Nantharat Phruksaphithak. Email: nantharat@tsu.ac.th.

Abstract: A new biocomposite was preformed between bacterial cellulose (BC) pellicle and polyethylene glycol (PEG) at different concentrations (0%, 5, 10%, 15% and 20%) and different molecular weight (600, 1000 and 2000). The structure and mechanical properties of BC/PEG biocomposite were investigated. The results indicated that the properties of the BC were improved by the addition of PEG. The morphology of the BC and BC/PEG blend was examined by a scanning electron microscope (SEM). These showed that PEG was coated with a large pore size fibril on the BC and the BC/PEG was dense with an even and smooth surface. All the Fourier transform infrared spectroscopy (FT-IR) thermograms of BC/PEG showed the same functional groups as typical BC and PEG. The DSC result showed that the thermal stability improved which might be associated with a weak interaction between BC and PEG, and may be useful for applications.

Keywords: Bacterial cellulose; poly (ethylene glycol); oil palm shoot juices

1 Introduction

Cellulose $(C_6H_{10}O_5)_n$ is a linear natural biocomposite and an organic compound comprised of a glucose unit linked by β(1,4)-glycosidic. Generally, it is isolated from vascular plants [1]. Many microorganisms, including bacteria, algae, and fungi, are also able to produce extracellular cellulose as an alternative natural resource [2]. This is called bacterial cellulose (BC). In fact, plant cellulose shows the same chemical formula as BC. But, BC displays higher purity than plant cellulose because it does not contain hemicellulose or lignin and extractive. The BC structure displays three-dimensional porous structures because of a hydrogen bonding-stabilized framework [3]. As a consequence, BC exhibits a higher crystallinity, ultrafine network structure, higher water absorption, higher mechanical strength and stronger biological adaptability in the wet state than plant cellulose [2,4,5]. As an extraordinary benefit of BC, it is easy to get the property-controlling fiber network and pore system modified, which is formed by self-assembly of the cellulose molecules in situ utilizing additives during biosynthesis. Nevertheless, a disadvantage for modification of BC is that it has plenty of water volume being effortlessly discharged under meager pressure, thus making BC easily dehydrated. Noticeably, there is some enhancement of biocomposite BC sheets, films, and gels over BC concerning mechanical attributes, biological function, and biomedical utilization [6]. The decrease of pore size was found to be attributed to the addition of polyethylene glycol (PEG) [7]. There are a variety of unique properties of BC gels, such as being soft, translucent, biocompatible, and water-retaining. Consequently, BC gels have been prevalently utilized as potential soft materials in the medical, cosmetic and food industries [8,9].

PEG is a polyether polymer synthetic having unique properties and applications in biotechnology and medicine. PEG is highly soluble and insufficient for volatility. Besides, its physical solubility has high hydrophilic properties; however, not only is it soluble in water, but also in many organic solvents. It has effectively been utilized to “camouflage” proteins from immune observation. PEG is regarded as a

DOI: 10.32604/jrm.2019.00020

compound being highly ubiquitous in many industries. For example, it is prevalently utilized in the pharmaceutical industry as a carrier for tiny molecule medicine or as an amphiphilic copolymer used in drugs for treating cancer. Moreover, toxicity, immunogenicity, and antigenicity are rarely found in PEG. Because of its contributing biocompatibility, it has been generally utilized in the medical industry so that the circulation time of drugs can be enhanced along with coating implants [2,6,10]. PEG is also inexpensive and significantly less hazardous than other organic solvents [11]. In addition it has hydrophilicity and thermal stability in the membranes [12]. As a result, PEG is widely used in industrial applications since its physical properties vary with its molecular weight (Mw). BC/PEG biocomposite is expected to be applied as biocomposite materials with enhanced properties relative to typical BC. Notwithstanding, it is effortless to discharge the PEG in BC/PEG biocomposite, providing it is in the context of slight pressure. Likewise, meager mechanical attributes are shown by BC/PEC due to the fact that the PEG is incapable of merging to the BC via a strong bonding, as a covalent bond. It is thus necessary to improve the mechanical properties of this biocomposite [6]. In this paper, we are reporting the characterization of BC/PEG biocomposite with different proportions of the concentration of PEG (5%, 10%, 15% and 20%) and Mw of PEG (PEG600, PEG1000 and PEG2000). Moreover, the BC was produced by *Acetobacter xylinum* TISTR 086 by consuming sugar or carbohydrates from oil palm shoot juice as their main food. The present paper clearly describes their morphology, crystallinity, mechanical and thermal properties.

2 Experimental Section

2.1 Materials

Bacterial cellulose (BC) was produced by strain *Acetobacter xylinum* TISTR 086, which was obtained from the Thailand Institute of Scientific and Technological Research (TISTR). Polyethylene glycol (PEG) (Mw of 600, 1000 and 2000) and sodium hydroxide were purchased from Sigma-Aldrich.

2.2 Preparation of BC Pellicles

The bacterium was cultured on oil palm shoot juices (OPSJ) and coconut juice (CJ) medium in a ratio of 50:50 v/v. BC was produced by *Acetobacter xylinum* TISTR 086 in tray (42 × 20 cm^2) at room temperature (27-30°C) for 10 days. After incubation, the pellicle produced on the surface of the media containing OPSJ and CJ medium was removed to eliminate the microbial cells. Distilled water was responsible for cleansing the pellicles with, 4% (w/v) sodium hydroxide solution in a heating bath (20 minutes) [13].

2.3 Preparation Biocomposite of BC/PEG (Mw 600, 1000 and 2000 g/mol)

The wet BC pellicle was expelled to remove some of the free water. Then, 1.00 of BC g was mixed with 0%, 5%, 10%, 15% and 20%(v/v) of PEG Mw 600, 1000 and 2000 (PEG600, PEG1000, and PEG2000). Then, BC was immersed in a 5 mL PEG aqueous solution for 24 h at room temperature. Distilled water was responsible for cleansing the surface of biocomposite BC so as to eliminate excessive PEG. All biocomposite BC were dehydrated at 70°C for 24 h or until final weight balanced constants in a naturally open atmosphere on a glass plate, then it was kept in desiccators before being characterized.

2.4 Composite Characterization

To evaluate the chemical structures, a Fourier transform infrared spectroscopy (FT-IR) was used. The biocomposite sample was cut into small pieces and a characterization of the function group of BC was performed using FT-IR in the mode attenuated total reflectance (ATR). All spectra were collected with a resolution of 4 cm^{-1} and 32 scans in the spectra range of 4000-400 cm^{-1} at room temperature.

The morphology of the surface and cross-section of the biocomposite were observed by a Field Emission Scanning Electron Microscope (FE-SEM) (Quanta400, FEI, Czech Republic) after gold coating. SEM with field emission gun and accelerating voltage at 3 kV was used to collect FE-SEM images.

The DSC data of biocomposite samples were recorded using a Perkin-Elmer DSC7 series (USA). A sample in a sealed aluminum pan was heated from 25°C to 400°C at a heating rate of 10 °C/min and a cooling rate of 5 °C/min under a constant stream of nitrogen (20 mL/min).

Shore hardness was tested according to (Shore A) ASTM D2240, ISO/R868, and JIS R7215 standards for biocomposites.

An X-ray diffractometer (Panalytical) was utilized to analyze X-ray diffraction (XRD) patterns, by means of Cu K_α radiation at 40 kV and 30 mA. The data scattering angle was noted, ranging from 5-40°. XRD data calculated the crystallinity according to Segal's equation [14].

$$\mathrm{CrI} = \frac{I_{200} - I_{am}}{I_{200}} \times 100 \quad (1)$$

where CrI = the crystalline index, I_{200} = the intensity at (200) peak ($2\theta = 22.3°$) and I_{am} = the minimum intensity between (100) and (200).

3 Results and Discussion

Generally, CJ is coconut water waste generated from the coconut industry to produce nata de coco for Thai desserts. Oil palm shoot is one of the most abundantly available oil palm waste produced after 20-25 years of growing [15]. However, the utilization of oil palm shoot for BC production was not reported. Oil palm shoot juice (OPSJ) is water that is squeezed out of the oil palm shoot and contains many sugars as shown in Table 1 that could be used as new alternative carbon sources for enhancing production of BC.

Table 1: The composition of sugar in OPSJ and CJ

Source	Sugar (g/L)				pH
	Glucose	Fructose	Sucrose	Total	
CJ	6.69	9.74	7.32	23.75	5.22
OPSJ	3.13	5.02	1.73	9.88	5.36

In our previous study, BC was capable of being obtained by *Gluconacetobacter xylinus* utilizing a mixture of OPSJ and CJ in a ratio of 50:50 v/v as a carbon source. This BC displayed a high Mw of 503,233 and a yield of 4.70 ± 0.11 g/L. While, the other mixture ratio of OPSJ and CJ showed a low yield and Mw of BC [13]. In general, BC has a large number of water molecules both on the surface and internal matrix caused by BC with an abundance of pores and various dimensions [16]. Furthermore, more porous BC can also absorb various substrates in a solution [17]. If the water in BC is not cleared away by evaporation, BC as a soft polymer transforms into a rigidity thin film by the irrevocable formation of new hydrogen bonds between cellulose hydroxyl groups. Therefore, these studies present treatment for BC derived from *Gluconacetobacter xylinus* with PEG aqueous solution (Mw 600, 1000 and 2000) by submerging the BC pellicle in PEG aqueous solution. After BC was treated with PEG, PEG slowly penetrated into the BC networks and when the surrounding water of polyglucosan chains was substituted with PEG, it led to the formation of bonds between hydroxyl groups of BC and PEG. In addition, PEG was able to coat the surface of BC as a structure model of BC/PEG composite as shown in Fig. 1. All these reasons caused BC to become softer.

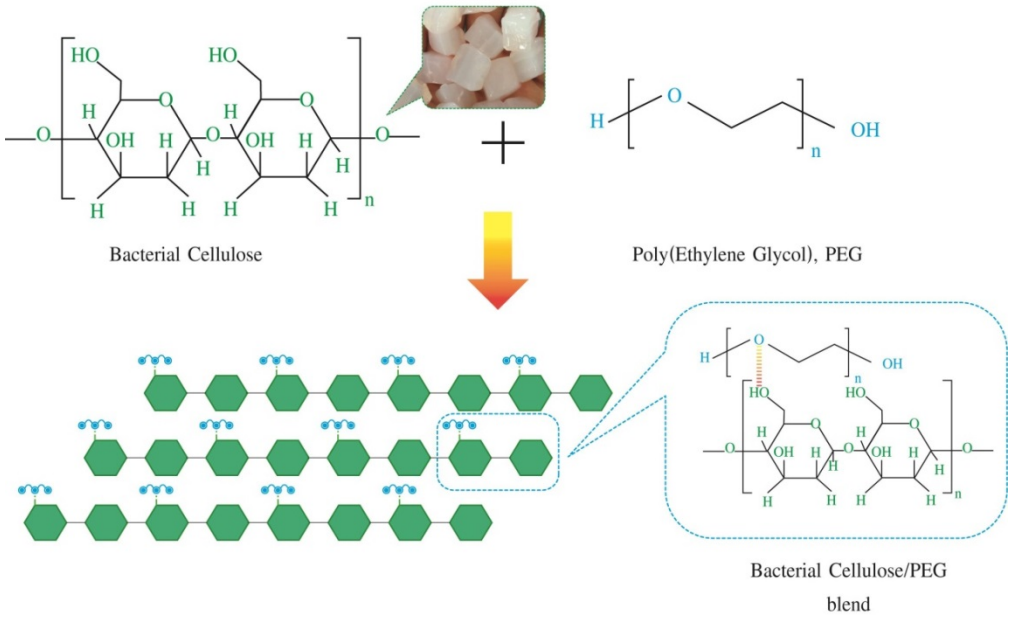

Figure 1: Structure model of the BC and the BC/PEG biocomposites

3.1 ATR-FTIR Spectroscopic Investigation

In order to determine the effect of PEG on the BC chemical structure, the FTIR spectra were analyzed in a wavenumber range of 650-4,000 cm^{-1} as shown in Fig. 2. The predominant absorption spectrum band of BC appeared at ~3,375 cm^{-1} and was assigned to -OH stretching vibration. The absorption band at ~2,900 cm^{-1} was assigned to C-H aliphatic stretching vibrations of alkane and asymmetric of CH_2 stretching which was supported by bending vibration at ~1,450 cm^{-1} [18]. The absorption band at 1,650 cm^{-1} was assigned to –OH bending vibration. The strong absorption band at 1,110 cm^{-1} was assigned to C-O-C stretching vibrations within the anhydroglucose ring. The small sharp band at ~900 cm^{-1} was assigned to the C-1 group, which had an absorption peak of β-glycosidic linkages between the sugar units. Then the different ratios of PEG (5% and 20%) blended with BC and the BC/PEG spectrum showed different wavenumbers between BC and BC/PEG biocomposite as presented in Fig. 2 to denote that BC and PEG have good intermolecular force as they are miscible or compatible. In case of PEG concentration increases 5% up to 20% (Figs. 2(A), 2(B) and 2(C)), the band of BC/PEG composite at 3,200-3,650 cm^{-1} as assign-OH stretching vibration became a broad peak due to the PEG having lots of hydroxyl group and the boarding of this band due to the merging of the peak for hydrogen bonding of both hydroxyl functionalized BC and the electronically charged PEG [2,17]. While the small peak intensity of ~2900 cm^{-1} and ~1450 cm^{-1} in BC/PEG became a clear shape peak result of the increase of C-H aliphatic of PEG [19]. Likewise, the assignment frequency at ~1100 cm^{-1} also presented board peak due to the C-O-C linkage [2,20]. As was seen, the ~950 cm^{-1} peak grew linearly with the concentration increasing PEG in BC. All wavenumber changes between BC and BC/PEG indicate that the intermolecular interaction of hydrogen bonds occurred throughout the hydroxyl group of BC and PEG. However, FTIR spectrums of BC/PEG600 and BC/PEG 1000 showed a similar spectrum change as BC/PEG2000.

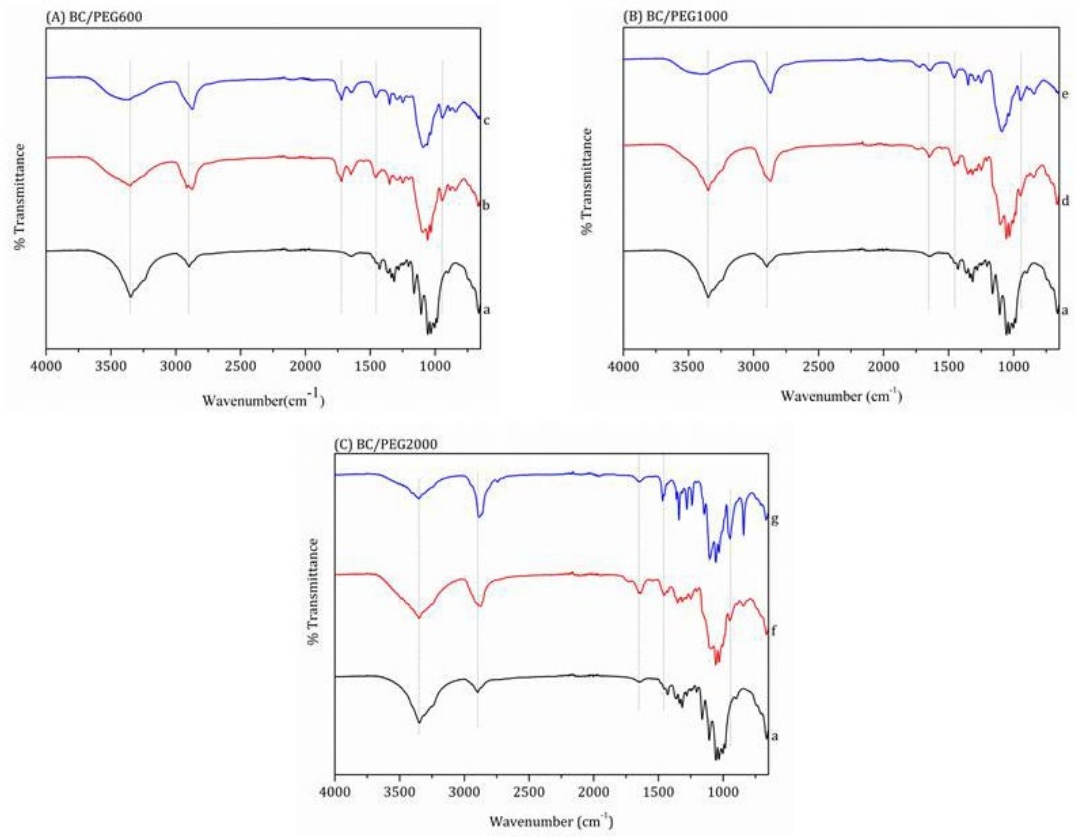

Figure 2: FTIR spectra of (A) BC/PEG600, (B) BC/PEG1000, and (C) BC/PEG2000 biocomposite: (a) BC, (b)BC/5PEG600, (c) BC/20PEG600, (d) BC/5PEG1000, (e) BC/20PEG1000, (f) BC/5PEG2000 (g) BC/20PEG2000

3.2 Shore Hardness Test (Shore A)

The hardness of dried BC and all BC/PEG biocomposite were examined according to the Shore A ASTM D2240 standard method as shown in Fig. 3. The data in these figures demonstrate the effect of the Mw and ratio of PEG on the hardness value of BC/PEG composite. The hardness value of neat BC was 52 Shore A, more rigid and brittle than wet BC. Then, PEG600, PEG1000 and PEG2000 blended with BC showed that hardness evidently increases (~6.0%) with PEG 2000 blending (BC became weaker). While PEG600 and PEG1000 blending with BC showed that the hardness was reduced (BC became softer) to 15% and 9%, respectively. Two factors may explain the possible effects of the hardness on the BC/PEG composite: intermolecular force and crystallinity. In the case of PEG600 as short chain PEG, it had low crystallinity, Van der Waal force as an intermolecular force and entanglement [19]. For the case of PEG1000 and PEG2000, there was a slight increase in crystallinity and a strong Van der Waal force between PEG and BC that led to an increase in the hardness properties of the BC/PEG composite. Therefore, our research indicates that PEG improved the hardness of dried BC.

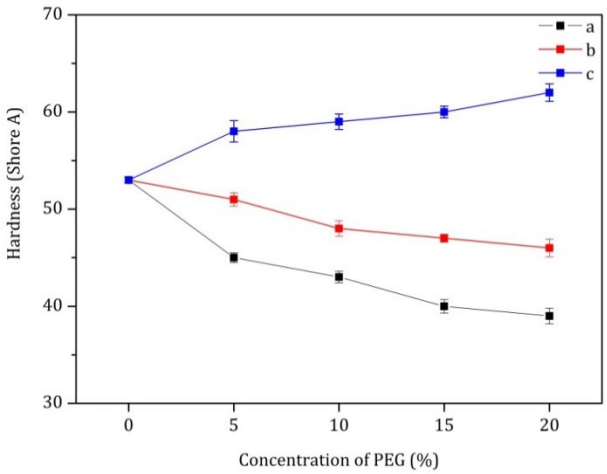

Figure 3: Hardness test of (a) BC/PEG600, (b) BC/PEG100, and (c) BC/PEG2000 biocomposite

3.3 Scanning Electron Microscopy (SEM)

The surface and cross-sectional morphologies of dried BC and the BC/PEG biocomposite were investigated using SEM as shown in Fig. 4. Fig. 4(A) shows the surface morphology of BC. The fibrils are randomly tightly packed to form a network structure without a bacterial cell. Fig. 5(A) shows a SEM micrograph of a cross-section of a BC sheet [2]. These show a uniform layer and empty spaces between layers were also noticed. To evaluate the diffusion of the different Mw of PEG (PEG600, PEG1000, and PEG2000) in BC, SEM of the surface and cross-section of BC/PEG biocomposites were carried out and the results are shown in Figs. 4(B) to 4(G) and Figs. 5(B) and 5(G), respectively. It can be seen that PEG significantly affected the morphology of BC. The surface of biocomposite was densely adhered, relatively smooth and had no obvious aggregation. This indicated the uniform distribution of PEG in the BC matrix as shown in Figs. 4(B)-4(G). Moreover, these figures show low Mw PEG is more miscible with BC than high Mw PEG. The cross-sectional morphology also showed a successful combination of PEG into the inside of BC as can be clearly seen in Figs. 5(B)-5(G). The gap between the layers of BC was decreased with PEG loading, which led to a bond formation between BC and PEG. Additionally, increasing the Mw of PEG600 to PEG2000 also decreased the gap between the layers. PEG600 and PEG1000 were more compatible with BC than PEG2000 because adhesion of PEG to the cellulose fibril surface was assumed to be related to the interaction force between the hydroxyl groups of BC and PEG.

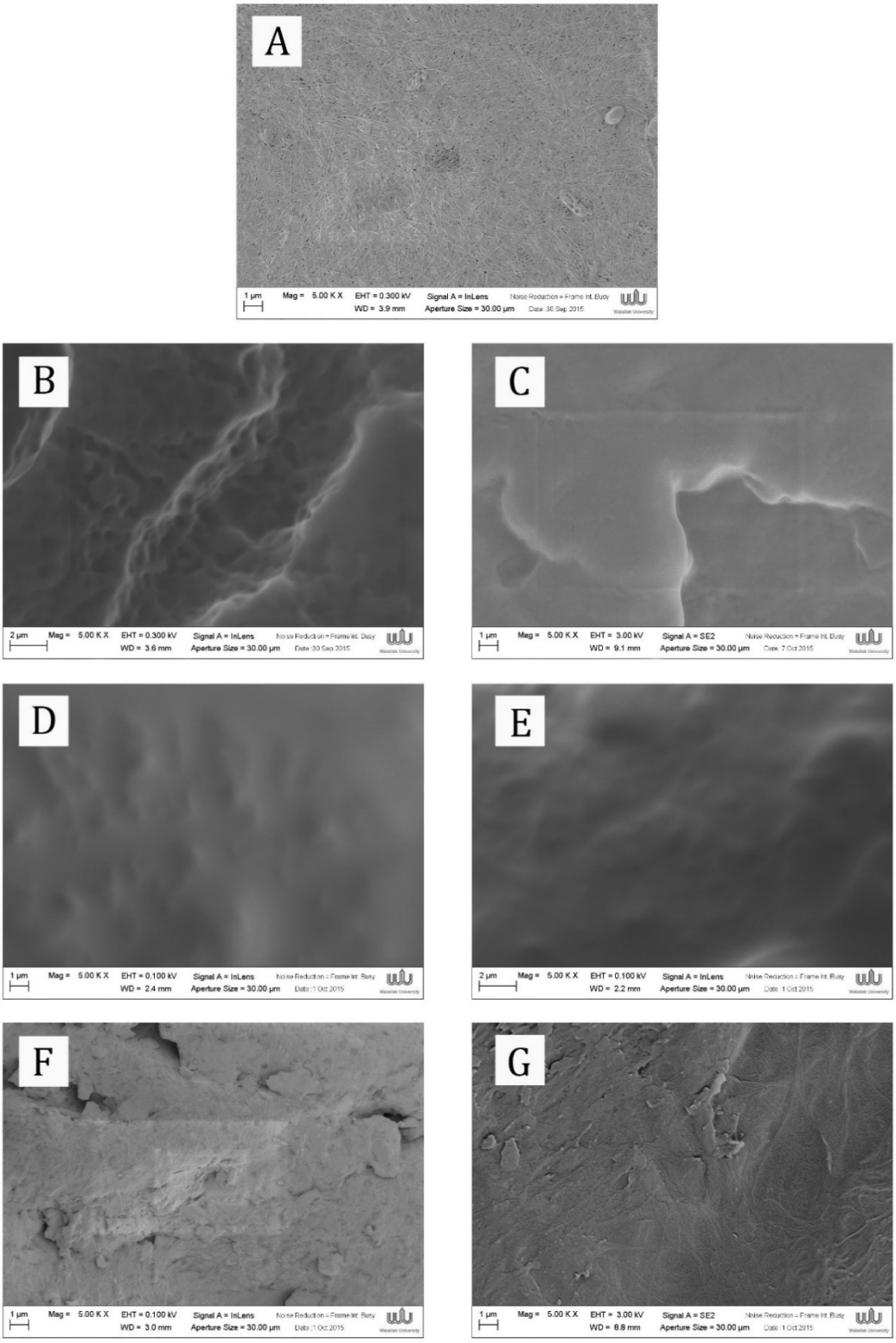

Figure 4: Effect of Mw and concentration of PEG on the surface morphology of (A) BC, (B)BC/5PEG600, (C) BC/20PEG600, (D) BC/5PEG1000, (E) BC/20PEG1000, (F) BC/5PEG2000 (G) BC/20PEG2000

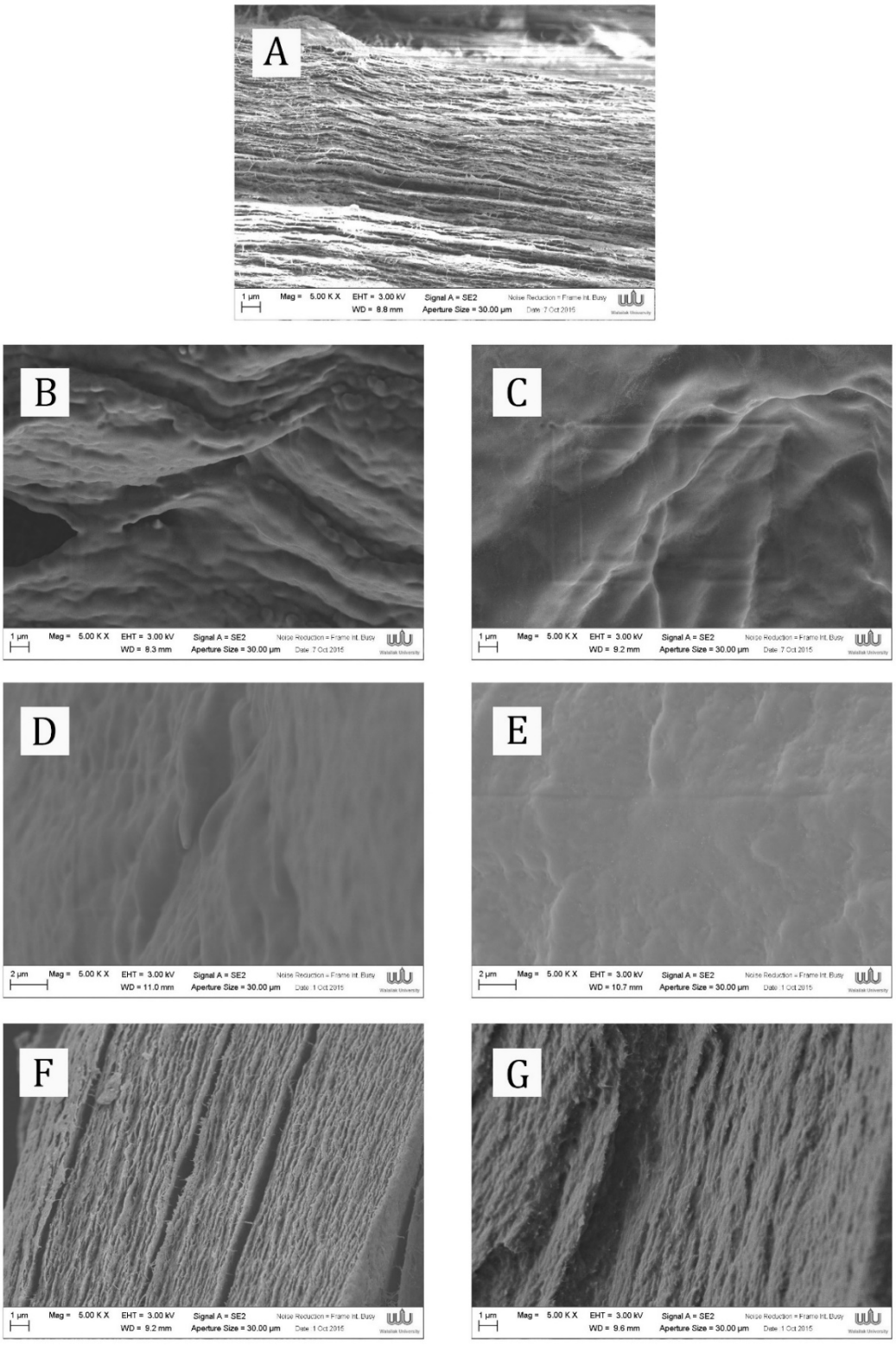

Figure 5: Effect of Mw and concentration of PEG on the cross-sectional morphology of (A) BC, (B)BC/5PEG600, (C) BC/20PEG600, (D) BC/5PEG1000, (E) BC/20PEG1000, (F) BC/5PEG2000 (G) BC/20PEG2000

3.4 Differential Scanning Calorimetry (DSC)

Fig. 6 displays DSC thermograms from the second heating of BC and BC/PEG composite being evaluated from 25 to 400°C at a heating rate of 10°C/min and a cooling rate of 5 °C/min under a constant stream of nitrogen (20 mL/min). The values of glass transition temperature (Tg) and melting temperature (Tm) of BC and BC/PEG composite are reported in Tab. 2. DSC thermogram of BC displayed an endothermic peak in the range of 140-160°C. This is ascribed to the removal of moisture, humidity, or other volatiles presented in the BC matrix (Fig. 6(a)). The second endothermic peak of Tg was around 230-260°C with the removal of tiny molecular fragments such as hydroxyl and methyl hydroxyl groups [21] corresponding to the volatilization stages of thermally degraded cellulose [22] (Fig. 6(a)). The small broad peak in the range of 345-360°C (not shown data) is due to a decomposition of the samples; a degradation of cellulose, dehydration, and decomposition of glucose units, transforming to become a carbon residue [23]. The state of PEG in the BC structure was investigated to evaluate the miscibility and interaction between the two polymers in thermal transition; Tg and Tm were also studied. The results of thermal properties at PEG concentration constant (BC/5PEG600, BC/5PEG1000, and BC/5PEG2000 composite) are shown in Fig. 6(A). The Tg of BC/5PEG600 composite slightly increased from 163°C to 167°C and 184°C of BC/5PEG1000, BC/5PEG2000, respectively. These results show that low Mw PEG is more miscible with BC than high Mw PEG [24] and low Mw of PEG influences Tg of BC [25] due to small molecule size and molecule chains with easy movement. In the case of increased PEG concentration (Fig. 6(B)), the Tg of the composite decreased and a broad peak formed due to PEG molecule having a weak interaction with the BC that reduced the mobility of the chain segment. While Tg of BC/20PEG600 composite was not reduced to lower Tg than BC/5PEG600. In the case of Tm, there is some literature on Tm of pure PEG600, PEG1000, and PEG2000 of 17°C [25], 40.7°C and 56.8°C [24], respectively. The Tm of BC/PEG600 composite and BC/PEG1000 were absent during the thermal scanning process (Figs. 6(A) (b and c), 6(B) (e and f)), indicating that PEG600 and PEG1000 exhibit a liquid state in the biopolymers and that PEG2000 promotes a crystalline to amorphous transition at higher levels of temperatures than those of the melting point. This suggests that PEG2000 has a thermodynamics impact on BC [22,26].

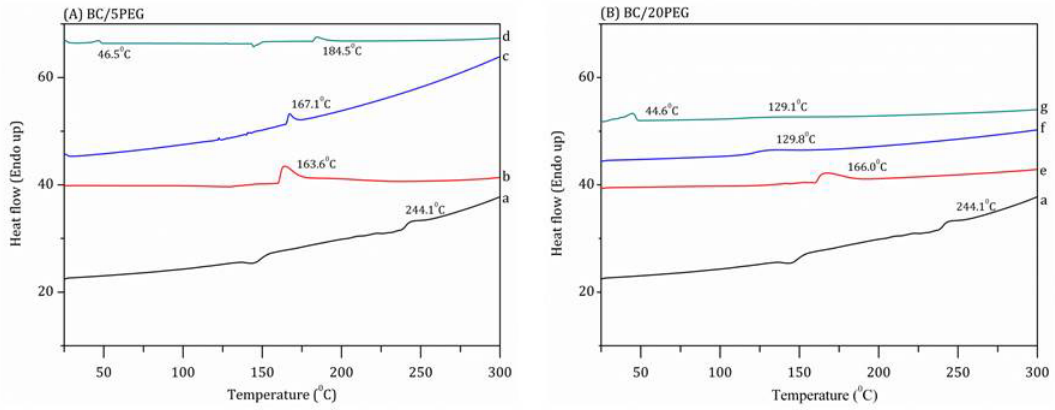

Figure 6*:* DSC thermogram of modified BC pellicles using at (A) BC/5PEG composite ((a) BC, (b) BC/5PEG600, (c) BC/5PEG1000, and (d) BC/5PEG2000) and (B) BC/20PEG composite ((e) BC/20PEG600, (f) BC/20PEG1000, and (g) BC/20PEG2000)

Table 2: T_g and T_m data of BC and BC/PEG composite from DSC thermogram

Composite	T_g (°C)	T_m (°C)
BC	244.1	353.0
BC/5PEG600	163.6	-
BC/5PEG1000	167.1	-
BC/5PEG2000	46.5	184.5
BC/20PEG600	166.0	-
BC/20PEG1000	129.8	-
BC/20PEG2000	44.6	129.1

3.5 X-ray Diffraction Analysis

The XRD patterns of the dried BC, BC/5PEG1000, and BC/5PEG2000 samples are shown in Fig. 7. The XRD pattern of BC shows three typical diffraction peaks for the following planes: at 2θ = 14.72° corresponding to the (101) reflection, 2θ = 16.74° corresponding to the (110) reflection and at 2θ = 22.75° corresponding to the (002) reflection. These define the crystalline form of cellulose-I [1,17]. Meanwhile, PEG demonstrates two main diffraction peak at about 18.9 and 23.1° [19,24,27]. The positional changes in the BC/PEG composite demonstrate that PEG has high chemical compatibility by blending. However, the XRD patterns of the BC/5PEG1000 and BC/5PEG2000 composites show a homogeneous structure [1,17,28], similar to the XRD patterns of BC.

Obviously, the main difference found between BC and BC/PEG composite is the peak intensity and degree of crystallinity as calculated by Segal's equation. These show that the estimated crystallinity of BC, BC/PEG1000, and BC/PEG2000 were 81.81%, 73.68%, and 85.71%, respectively. These results display that the presence of low Mw PEG had an effect on the decrease of the peak intensity of BC due to it having a short chain and less hydrogen bonding that weakened the interaction between BC and also the coating space between BC, which completely reduced its crystallinity [2,19]. On the other hand, the high Mw PEG had a long chain that sustained the PEG chain in the BC matrix. These had mobility and orderly rearrangement leading to the high crystallinity of BC/5PEG2000 composite. The XRD results were in agreement with previous studies on hardness test Title 3.2.

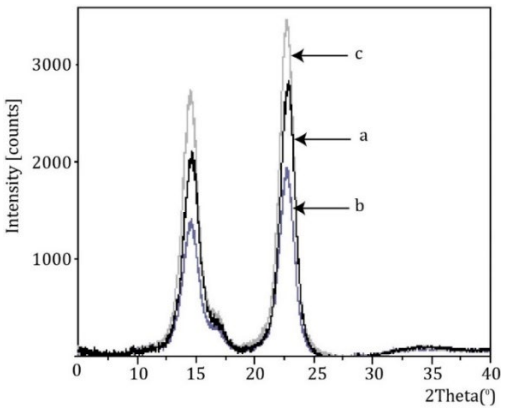

Figure 7: X-ray diffraction patterns for (a) BC, (b) BC/PEG1000 and (c) BC/PEG2000 composite

4 Conclusions

In this study, BC was produced by *Acetobacter xylinum* TISTR 086 by consuming sugar or carbohydrates from oil palm shoot juice as their main food. Then BC biocomposite was successfully prepared by immersing wet BC pellicle in PEG600, PEG1000, and PEG2000 aqueous solutions and different concentrations of PEG (5, 10, 15, and 20). The development of BC/PEG biocomposite materials by in situ modification depends on the Mw and concentration of PEG. As Mw of PEG and concentration increase, they have an effect on the depression of the miscible and thermo-mechanical properties of the BC/PEG composite due to the length of the polymer chain and interaction molecular force. Hence, the Mw of PEG plays an important or key role regarding the concentration of PEG. However, for this research, the Mw of PEG1000 was chosen as the optimum level to develop the mechanical properties of BC. Because BC and PEG are clearly miscible, hardness and Tg of dried BC decreased, which provide more opportunity for its wide application in the food industry or tissue engineering in the near future.

Acknowledgements: This work was supported by financial support from the Thaksin University Research Fund in 2015, Microbial Resource Management Research Unit, Department of Biology and Department of Chemistry, Thaksin University, Thailand.

References

1. Velmurugan, P., Myung, H., Govarthanan, M., Yi, Y. J., Seo, S. K. et al. (2015). Production and characterization of bacterial cellulose by *Leifsonia* sp. CBNU-EW3 isolated from the earthworm, *Eisenia fetida*. *Biotechnology and Bioprocess Engineering, 20(3),* 410-416.
2. Cai, Z., Kim, J. (2010). Bacterial cellulose/poly(ethylene glycol) composite: characterization and first evaluation of biocompatibility. *Cellulose, 17(1),* 83-91.
3. Zhou, T., Chen, D., Jiu, J., Nge, T. T., Sugahara, T. et al. (2013). Electrically conductive bacterial cellulose composite membranes produced by the incorporation of graphite nanoplatelets in pristine bacterial cellulose membranes. *eXPRESS Polymer Letters, 7(9),* 756.
4. Castro, C., Zuluaga, R., Alvarez, C., Putaux, J. L., Caro, G. et al. (2012). Bacterial cellulose produced by a new acid-resistant strain of *Gluconacetobacter* genus. *Carbohydrate Polymers, 89(4),* 1033-1037.
5. Tanskul, S., Amornthatree, K., Jaturonlak, N. (2013). A new cellulose-Producing bacterium, Rhodococcus sp. MI 2: Screening and optimization of culture conditions. *Carbohydrate Polymers, 92(1),* 421-428.
6. Sabir, A., Shafiq, M., Islam, A., Sarwar, A., Dilshad, M. R. et al. (2015). Fabrication of tethered carbon nanotubes in cellulose acetate/polyethylene glycol-400 composite membranes for reverse osmosis. *Carbohydrate Polymers, 132,* 589-597.
7. Hebler, N., Klemm, D. (2009). Alteration of bacterial nanocellulose structure by in situ modification using polyethylene glycol and carbohydrate additives. *Cellulose, 16(5),* 899-910.
8. Chawla, P. R., Bajaj, I. B., Survase, S. A., Singhal, R. S. (2009). Microbial cellulose: fermentative production and applications. *Fermentative Production and Applications, 47(2),* 107-124.
9. Shah, N., Ul-Islam, M., Khattak, W. A., Park, J. K. (2013). Overview of bacterial cellulose composites: a multipurpose advanced material. *Carbohydrate Polymer, 98(2),* 1585-1598.
10. Liang, M. T., Liang, R. C. (2012). Fractionation of polyethylene glycol particles by simulated moving bed with size-exclusion chromatography. *Journal of Chromatography A, 1229,* 107-112.
11. Vafaeezadeh, M., Hashemi, M. M. (2015). Polyethylene glycol (PEG) as a green solvent for carbon-carbon bond formation reactions. *Journal of Molecular Liquids, 207(3),* 73-79.
12. Numata, Y., Sakata, T., Furukawa, H., Tajima, K. (2015). Bacterial cellulose gels with high mechanical strength. *Materials Science and Engineering: C, 47,* 57-62.
13. Phruksaphithak, N., Kaewnun, C., Thong, S. O. (2017). Productions and properties of bacterial cellulose from oil palm shoot juices felled medium and coconut medium. *Key Engineering Material, 728,* 271-276.
14. Yang, Y., Jia, J., Xing, J., Chen, J., Lu, S. (2013). Isolation and characteristics analysis of a novel high bacterial cellulose producing strain Gluconacetobacter intermedius CIs26. *Carbohydrate Polymers, 92(2),*

2012-2017.

15. Sulaiman, O., Salim, N., Nordin, N. A., Hashim, R., Ibrahim, M. et al. (2012). The potential of oil palm trunk biomass as an alternative source for compressed wood. *Bioresources, 7(2),* 2688-2706.
16. Santos, S. M,, Carbajo, J. M., Quintana, E., Ibarra, D., Gomez, N. et al. (2015). Characterization of purified bacterial cellulose focused on its use on paper restoration. *Carbohydrate Polymers, 116,* 173-181.
17. Khan, S., Ul-Islam, M., Khattak, W. A., Ullah, M. W., Park, J. K. (2015). Bacterial cellulose-poly(3,4-ethylenedioxythiophene)-poly(styrenesulfonate) composites for optoelectronic applications. *Carbohydrate Polymers, 127,* 86-93.
18. Ul-Islam, M., Shah, N., Ha, J. H., Park, J. K. (2011). Effect of chitosan penetration on physico-chemical and mechanical properties of bacterial cellulose. *Korean Journal of Chemical Engineering, 28(8),* 1736-1743.
19. Sun, G., Zhang, X. Z., Chu, C. C. (2008). Effect of the molecular weight of polyethylene glycol (PEG) on the properties of chitosan-PEG-poly(N-isopropylacrylamide) hydrogels. *Journal of Materials Science: Materials in Medicine, 19(8),* 2865-2872.
20. Kumar, T. (1990). Fourier transform infrared spectrometric determination of polyethylene glycol in high-density polyethylene. *Analyst, 115(12),* 1597-1599.
21. Cheng, K. C., Catchmark, J. M., Demirci, A. (2009). Enhanced production of bacterial cellulose by using a biofilm reactor and its material property analysis. *Journal of Biological Engineering, 3(12),* 1-10.
22. Kiziltas, E. E., Kiziltas, A., Gardner, D. J. (2015). Synthesis of bacterial cellulose using hot water extracted wood sugars. *Carbohydrate Polymers, 124,* 131-138.
23. Mohammadkazemi, F., Azin, M., Ashori, A. (2015). Production of bacterial cellulose using different carbon sources and culture media. *Carbohydrate Polymers, 117,* 518-523.
24. Li, Y., Ma, Q., Huang, C., Liu, G. (2013). Crystallization of poly (ethylene glycol) in poly (methyl methacrylate) networks. *Materials Science (MEDŽIAGOTYRA), 19(2),* 147-151.
25. Oh, H. J., Freeman, B. D., McGrath, J. E., Lee, C. H., Paul, D. R. (2014). Thermal analysis of disulfonated poly(arylene ether sulfone) plasticized with poly(ethylene glycol) for membrane formation. *Polymer, 55(1),* 235-247.
26. Liu, X., Jiang, Z., Han, J. (2011). Influence of adding different poly(ethylene glycol) in the biosynthesis of bacterialc. *Advanced Materials Research, 418-420,* 589-592.
27. Wen, R., Jia, P., Huang, Z., Fang, M., Liu, Y. et al. (2018). Thermal energy storage properties and thermal reliability of PEG/bone char composite as a form-stable phase change material. *Journal of Thermal Analysis and Calorimetry, 132(3),* 1753-1761.
28. Liang, S., Wu, J., Tian, H., Zhang, L., Xu, J. (2008). High-strength cellulose/poly(ethylene glycol) gels. *Chemistry and Sustainability, Energy and Materials, 1(6),* 558-563.